Dynamic MRI-based computer aided diagnostic systems for early detection of kidney transplant rejection: A survey

Mahmoud Mostapha, Fahmi Khalifa, Amir Alansary, and Ahmed SolimanGeorgy Gimel'farbAyman El-Baz

Citation: AIP Conference Proceedings **1559**, 297 (2013); doi: 10.1063/1.4825022
View online: http://dx.doi.org/10.1063/1.4825022
View Table of Contents: http://aip.scitation.org/toc/apc/1559/1
Published by the American Institute of Physics

Dynamic MRI-Based Computer Aided Diagnostic Systems for Early Detection of Kidney Transplant Rejection: A Survey

Mahmoud Mostapha*, Fahmi Khalifa*, Amir Alansary*, Ahmed Soliman*, Georgy Gimel'farb† and Ayman El-Baz*

*BioImaging Laboratory, Bioengineering Department, University of Louisville, Louisville, KY, USA.
†Department of Computer Science, University of Auckland, Auckland, New Zealand.

Abstract. Early detection of renal transplant rejection is important to implement appropriate medical and immune therapy in patients with transplanted kidneys. In literature, a large number of computer-aided diagnostic (CAD) systems using different image modalities, such as ultrasound (US), magnetic resonance imaging (MRI), computed tomography (CT), and radionuclide imaging, have been proposed for early detection of kidney diseases. A typical CAD system for kidney diagnosis consists of a set of processing steps including: motion correction, segmentation of the kidney and/or its internal structures (e.g., cortex, medulla), construction of agent kinetic curves, functional parameter estimation, diagnosis, and assessment of the kidney status. In this paper, we survey the current state-of-the-art CAD systems that have been developed for kidney disease diagnosis using dynamic MRI. In addition, the paper addresses several challenges that researchers face in developing efficient, fast and reliable CAD systems for the early detection of kidney diseases.

Keywords: segmentation, registration, DCE-MRI, CAD, kidney, acute renal rejection
PACS: 01.30.Rr

INTRODUCTION

Early detection of kidney rejection is important for clinical management in patients with transplanted kidneys. In the United States, approximately 17,736 renal transplants are performed annually [1] and, given the limited number of donors, transplanted kidney salvage is an important goal. Renal transplantation complications can be divided into six categories [2]: *(i)* urologic complications (e.g., urine leaks, calculous disease and urinary obstruction); *(ii)* fluid collections (e.g., urinomas, hematomas, lymphoceles, and abscesses); *(iii)* vascular complications (e.g., artery stenosis, infarction, arteriovenous fistulas and pseudoaneurysms, and renal vein thrombosis), *(iv)* neoplasms (e.g., renal cell carcinomas and lymphomas), *(v)* recurrent native renal disease, and *(vi)* graft dysfunction (e.g., acute tubular necrosis (ATN), renal rejection, and drug toxicity).

Acute rejection, i.e., the immunological response of the human immune system to a foreign kidney, is the most important cause of renal dysfunction among other diagnostic possibilities. The incidence of renal rejection episodes depends on several factors, e.g., the organ (status), co-morbidities, medication and compliance [3]. Chronic allograft deterioration increases significantly with each acute rejection episode [4]. Consequently, early detection and effective-fast treatment of acute rejection are crucial to preserve a

2013 International Symposium on Computational Models for Life Sciences
AIP Conf. Proc. 1559, 297-306 (2013); doi: 10.1063/1.4825022

graft's function. At present, initial evaluation of renal dysfunction after transplantation is based on blood tests and urine sampling (e.g., plasma creatinine, creatinine clearance). However, these tests provide information on both kidneys together. Also, significant change in creatinine level is only detectable after the loss of 60% of the kidney function [5], which limits the efficiency of such indexes in detecting renal rejection. Nonetheless, biopsy remains the gold standard, but only as the last resort because of its invasive nature that may cause injury to the graft, high costs, and potential morbidity rates. Moreover, biopsy is limited to patients who are not taking any anticoagulant drugs and may lead to wrong estimation of inflammation extent as it relies on few small samples from limited areas to determine the status of the entire organ.

Noninvasive functional assessment of transplanted kidneys has been clinically explored with several imaging modalities. Radionuclide imaging (scintigraphy) is an excellent modality for evaluating graft function, both qualitatively and quantitatively, while screening for common complications. However, due to its limited spatial resolution, functional abnormalities inside different parts of the kidney (e.g., cortex and medulla) cannot be discriminated precisely [6]. Also, radionuclide imaging involves radiation exposure, thereby limiting the applicability of these techniques, especially in monitoring such diseases as ATN or cyclosporine A toxicity [7]. Ultrasound imaging (US) is a relatively cheap and non-nephrotoxic that is usually used in early postoperative period, as well as for long-term follow-up assessment of the transplanted kidney. However, it suffers from low signal-to-noise ratios, shadowing artifacts, speckles that greatly decrease image quality and diagnostic confidence. Computed tomography (CT) is commonly available technology that uses contrast agents. However, information gathered by CT to detect renal acute rejection is unspecific and the contrast agents used still are nephrotoxic. Therefore, currently CT has a limited role in diagnosing acute renal rejection [3]. Although magnetic resonance imaging (MRI) provides excellent morphological information that allowed advanced analysis of renal function, structural MRI lacks functional information. Dynamic contrast enhanced magnetic resonance imaging (DCE-MRI) has emerged as a new noninvasive technique to provide superior information of the anatomy, function, and metabolism of tissue [8]. Advantages of DCE-MRI techniques over other imaging modalities include the lack of ionizing radiation, increased spatial resolution, the ability to provide superior anatomical and functional information, and the feasibility to be used as early as possible (even one day post-transplantation) for the assessment and follow-up of the transplanted kidney. DCE-MRI involves the acquisition of serial MR images with high temporal resolution before, during, and several times after the administration of a contrast agent (e.g., gadolinium) into the blood stream. The gadolinium behaves as a leakage agent, namely it distributes in the extracellular extravascular space, and at short times (up to about 2 minutes) after administration at DCE-MRI, time-intensity curves (TIC) that represent the average intensity of the kidney can be constructed. From these TICs, empirical parameters (indexes) that reflect the delivery of agent to the tissue bed can be estimated (see Fig. 1). In this paper, we will focus on kidney diagnosis using DCE-MRI.

Developing a computer-aided diagnostic (CAD) system for early and noninvasive diagnosis of the kidney is an ongoing area of research interest. A schematic diagram of a typical CAD system for detection of acute rejection using DCE-MRI is shown in Fig. 2. The motion correction step of DCE-MRI times series is a preprocessing

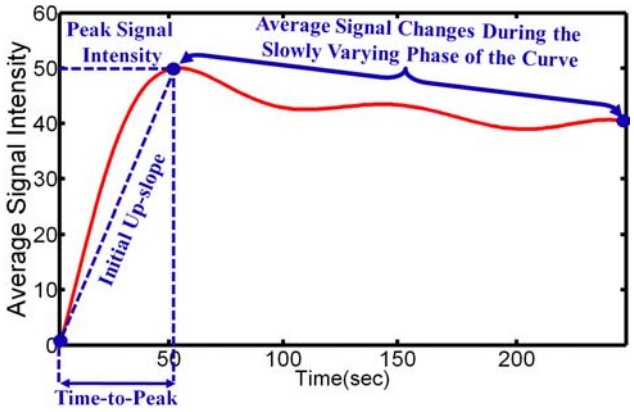

FIGURE 1: Typical TIC of a DCE-MRI time series data illustrating the transient (peak value, time to the first peak and the initial up-slope) and tissue distribution phases' parameters that can be estimated and used for diagnosis.

step to compensate for the global and/or local kidney motion. Next, kidney objects are segmented and the functional unit (i.e., cortex) is extracted in order to determine dynamic agent delivery. Finally, perfusion is estimated from contrast agent kinetics using empirical indexes (see Fig. 1) and classification/disgnosis of kidney status is performed using the extracted features. Below, we will overview the related work on renal image segmentation and registration as well as the today's CAD systems for kidney diagnosis using DCE-MRI.

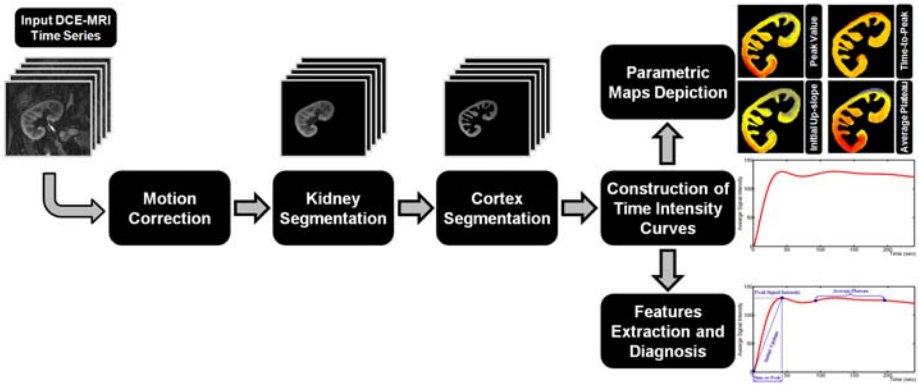

FIGURE 2. Typical computer-aided diagnosis (CAD) system for diagnosis of acute renal rejection. The input of a CAD system is the DCE-MRI medical images.

RENAL IMAGE SEGMENTATION AND REGISTRATION

Accurate segmentation and registration of dynamic MR renal images is a challenge due to the relatively low signal-to-noise, non-uniform signal intensity over the time series, and kidney deformations caused by gross patient motion, transmitted respiratory and pulsatile effects. Particularly, motion effects can be compensated for by using global and local registration methods. Kidney segmentation techniques can be classified into three main categories: threshold-based, deformable model-based, and probabilistic or energy minimization-based methods.

Threshold-based techniques segments the kidney and its internal structures (i.e., cortex and medulla) by analyzing an empirical probability distribution, or histogram of

pixel intensities in a region-of-interest (ROI). Earlier renal image analysis (e.g., [9–12]) was usually carried out either manually or semi-automatically. Typically, the user defines a ROI in one image and for the rest of the images, image edges were detected and the model curve was matched to these edges. However, this is subject to inter- and intra-observer variability, and valuable information inherent in the DCE-MRI signal intensity time series (sequences) is not used. Additionally, these approaches are very slow, even though semi-automated techniques (e.g., [9, 12]) do reduce the processing time. Giele et al. [13] introduced an approach for the kidney segmentation and registration. First, the kidney contour is drawn manually by the user in a single high-contrast image. Then, the phase difference movement detection (PDMD) method is employed to correct kidney displacements. Their method demonstrated better performance than image intensity matching and cross-correlation; however, the accuracy was about 68%, a manual mask was still required, and only translational motion was handled. De Priester et al. [12] subtracted the average of pre-contrasted images (10 frames) from the average of early-enhanced images (30 frames) and thresholded the resulting difference image to obtain a kidney mask. Objects smaller than a certain size (700 pixels) were removed, and the remaining kidney object was closed using morphological erosion and manual processing. This approach was further expanded by Giele [14] by applying an erosion filter to the mask image in order to obtain a contour at a second subtraction stage. Koh et al.[15] segmented kidneys with the morphological 3D H-maxima transform. Rectangular masks and edge information are used to exclude training data or prior knowledge. Simple thresholding is too inaccurate to segment human organs in DCE-MRI, because these specific regions have similar gray levels distributions.

Evolving deformable boundary methods have been explored as a more accurate means of kidney segmentation. A series of studies on both rats and human subjects [16–19] have been conducted for the registration and segmentation of DCE-MRI. A multi-step segmentation and registration in the study on humans by Sun et al. [16, 17] initially corrects large scale motion by using a gradient-based similarity rigid registration. Once roughly aligned, a high-contrast image is subtracted from a pre-contrast image and a level set approach was used to extract the kidney from the difference image. Then, the segmented contour is propagated over other frames to search for the rigid (rotation and translation) registration parameters. For rat studies [18, 19], a variational level set approach that integrates a subpixel motion model and temporal smoothness constraints was used to find the kidney borders. For segmenting the cortex and medulla, the technique proposed by Chan and Vese [20] was used. Abdelmunim et al. [21] incorporated both image and shape prior information into a variational framework. However, their model did not adequately account for spatial dependencies between the pixels and therefore is quite sensitive to imperfect kidney contours and image noise. Yuksel et al. [22, 23] proposed a parametric deformable model approach for the segmentation of the kidney where the contour evolution was constrained using two density functions. The first describes a shape prior and is constructed using the average signed distance maps of the training samples. The second describes greylevel distribution of the kidney and its background, estimated using an adaptive linear combinations of discrete Gaussians (LCDG) [24, 25]. A similar approach that incorporated shape and visual appearance priors was proposed by El-Baz et al. [26]. Their shape model is constructed from a linear combination of vectors of distances between the training boundaries and their common centroid. The

appearance prior is modeled with a spatially homogeneous second-order Markov-Gibbs random field (MGRF) of gray levels with analytically estimated pairwise potentials. Khalifa et al. [27, 28] proposed a level set-based framework for kidney segmentation. The proposed a stochastic force [29] that accounts for a shape prior and features of image intensity and pairwise MGRF spatial interactions [30, 31]. They employed a two-stage registration methodology using an affine registration to account for the global motion, followed by a Laplace-based approach for local motion correction [29]. Gloger et al. [32] presented a level set-based approach using shape prior and Bayesian statistical concepts for shape probability maps generation. However, the shape prior model in [27, 32] did not impose temporal constraints on kidney segmentation.

The graph cut-based segmentation algorithm by Boykov et al. [33] minimizes an energy function of a temporal MGRF model of intensity curves. The results looked promising, but manual interaction was still required. Rusinek et al. [34] proposed a graph-cut based segmentation formwork to assess functional parameters. Their method employed a rigid registration step to account for the kidney displacements and the approach has been tested on simulated and in-vivo data. Ali et al. [35, 36] used the graph cut-based minimization of an energy functional combining a shape constraint with boundary properties. The constraint was built using a Poisson probability distribution and distance maps. Chevaillier et al. [37] proposed a semi-automated method to segment internal structures (i.e., cortex, medulla, and pelvis) from DCE-MRI time series by using *k*-means based partitioning to classify pixels according to contrast evolution using vector quantization algorithm. However, it was only tested on eight data sets for normal kidneys, and user interaction was still required. A similar segmentation by Song et al. [38] has only been tested on two MRI data sets, with simulated rotation and translation rigid motion, for one normal and one abnormal kidney. An automated framework proposed by Zöllner et al. [39] assesses renal function by deriving voxel-based functional information from DCE-MRI, the nonrigid image registration compensating for the motion and deformation of the kidney during DCE-MRI acquisitions. A *k*-means clustering method was used for extracting functional information about different regions of the kidney according to their dynamic contrast enhancement patterns. An automated wavelet-based k-means clustering framework for segmenting the kidneys was proposed by Li et al. [40]. The images were co-aligned using B-splines registration and cross-correlation (CC) cost function and their framework was tested on seven subjects (four volunteers and three patients). Yang et al. [41] proposed a framework for the classification of kidney tissue using fuzzy c-mean clustering. Their framework employed a nonrigid registration step using the demons algorithm [42] and the squared pixel distance as a similarity metric and the squared gradient of the transformation field as the smoothness regularization term.

DCE-MRI BASED RENAL CAD SYSTEMS

Recently, several CAD systems have been proposed to analyze kidney function using DCE-MRI. Farag et al. [43] and El-Baz et al.[44–47] proposed an automated framework for early diagnosis of acute renal transplant rejection. They designed an external energy function to control the deformable boundary evolution that accounts for two density estimations: one for a shape model and the other for gray level distribution estimated using linear combination of Gaussians (LCG) [30, 31, 48]. For local motion correction,

a geometric-based nonrigid registration approach that deforms the kidney objects over a set of closed equi-spaced contours) iso-contours was introduced. The evolution of the iso-contours is guided by an exponential speed function by minimizing the distances between the corresponding pixel pairs on the reference and target iso-contours. Their frameworks was tested on 30 datasets and the evaluation of the kidney status was based on four empirical parameters (peak signal intensity, time-to peak, the slope between the peak and the first minimum (wash-in slope), and the slope between the peak and the signal measured from the last image in the sequence (was-out slope). A similar CAD system was proposed in [49]. They employed a global alignment step based on maximizing a special Gibbs energy function, the perfusion curves were estimated from the whole kidney rather than the cortex, and the system was tested on a larger cohort of 100 patients. A semiautomated approach by Rusinek et al. [34] assessed cortical and medullary functional parameters (renal plasma flow (RPF), glomerular filtration rate (GFR), vascular volumes of the cortex and medulla, and rate of water absorption) using simulated and in-vivo data. Their framework employed an initial rigid alignment (translation only) step followed by a graph-cut based segmentation approach. Zikic et al. [50] evaluated kidney kinetic parameters after motion correction using template-matching based registration and normalized gradient field (NGF), as the contrast-invariant similarity measure. However, the kidney was segmented manually, only the translational motion was considered, and the evaluation of perfusion parameters (plasma volume and tubular flow) was performed visually by trained physicians for 10 data sets of healthy volunteers. Semiautomated evaluation of renal function was explored by De Senneville [51] using rigid registration to handle kidney motion inside a user-defined ROI. The renal cortex was segmented manually, and the GFR was estimated with Patlak-Rutland kinetic model. Their method demonstrated a significant uncertainty reduction on the computed GFR for native kidneys, but not the transplanted ones. Anderlik et al. [52] proposed a framework for quantitative assessment of kidney function using a two-step motion correction and pharmacokinetic modeling. The GFR was estimated from the TICs using the compartment model proposed by Sourbron et al. [53]. Their framework has been tested on 11 data sets. Zöllner et al. [39] employed a nonrigid registration using B-splines and mutual information (MI) as a similarity metric. Functional information was extracted regionally using k-means clustering. This system was tested only on four DCE-MRI data sets and the evaluation of kidney regions was assessed qualitatively according to their mean signal intensity time courses. An automated framework for the classification of kidney transplant status was proposed by Khalifa et al. [27, 28, 54]. In their framework, the kidney was segmented using a stochastic geometrical deformable model approach and the local motion of the kidney is corrected for by a Laplace partial differential equation-based nonrigid alignment method [29]. The system was tested on 26 data sets and the kidney status was evaluated using K-nearest neighbor classifier based on empirical parameters estimated from the agent kidney kinetic curves. Their framework was later extended in [54] by using analytical function-based model to fit agent kinetic curves derived from the cortex rather than the whole kidney as in [27]. For the classification of kidney status, five features (three are derived from the gamma-variate functional model and two are from the perfusion data, namely the time-to-peak and average plateau, see Fig. 1) were chosen, and the study included 50 transplant patients (27 non-rejection and 23 acute rejection). Semi-automated estimation of renal parameters was performed by Hodneland

et al. [55]. A viscous fluid model combined with an NGF-based cost function was used for elastic kidney registration. However, the kidney was segmented interactively with the nearest neighbor approach, the framework was tested only on 4 data sets of two healthy volunteers, and the reported GFR measurements were slightly underestimated relative to the creatinine reference values. Positano et al. [56] proposed a CAD system for the estimation for renal parameters. Their system included a two-step rigid registration framework to compensate for kidney motion using MI and adaptive prediction of kidney position over the course of the respiratory cycle. The perfusion indices (peak signal intensity, mean transit time (MTT), initial up-slope, and time to peak) was evaluated on perfusion curves extracted from the automatically and manually registered datasets were similar as well. However, their registration method could address only the global motion, but not the local motion.

DISCUSSION AND CONCLUSIONS

Efficient and reliable CAD systems for early detection of renal transplant complications are very important. This is due to the fact that early detection of renal complications, especially renal rejection, can be potentially increase the quality of a patient's post-transplant treatment. This paper overviews recent CAD systems for the detection of kidney rejection using dynamic contrast-enhanced magnetic resonance imaging (DCE-MRI), and addresses their strengths and limitations. However, several research challenges and aspects have been facing each stage of the development of accurate and fast CAD systems. These challenges can be summarized as follows:

- Most clinical and research studies focuses on 2D time series analyses that are compatible with data acquisitions for real patient scenarios. However, the extension to 4D (3D + time) is one of the major challenges. The goal of DCE-MRI is to obtain the most feasible temporal resolution, while maintaining good spatial resolution. Therefore, the acquisition of a 3D time series that has a higher spatial resolution greatly affects the temporal resolution, and vice versa. Thus, a compromise in choosing the acquisition parameters for 3D time series (4D) is required to achieve a sufficiently high signal-to-noise ratio, since acquiring ideal rapid isotropic 3D imaging of a moving kidney is not achievable [51].
- Accurate delineation of kidney borders requires new segmentation models to account for the large inhomogeneities in kidneys (i.e., cortex, medulla). This can be achieved by integrating spatial interactions between the kidney pixels or voxels that represent the kidney and the intensity information in the segmentation techniques. Most popular spatial interaction models are MGRF-based methods, using binary maps and pairwise relationships for 2D and 3D images (see e.g., [27, 29–31]). A recent study by Khalifa et al. [28] demonstrated the advantage of higher-order MGRF spatial model over second-order models for kidney segmentation from DCE-MRI. Also, a new trend in medical image analysis is to learn the appearance of the kidney using an MGRF trained on grey-scale images as opposed to binary maps [57–60].
- Motion artifacts present another major challenge for automated analysis of DCE-MRI. Both global and local kidney deformations affect accurate analysis of perfusion data. In literature, a tremendous number of image registration methods have

been proposed to handle both global and local motion in medical images [61]. A new trend to provide more accurate registration is the use of higher-order similarity metrics [62–64]. Unlike other registration methods that are prone to image intensity variations over the time series, other sophisticated methods [27, 44, 54] explicitly depends only on the geometric features to compensate for the kidney motion. These approaches can also be extended to deal with 3D data.

REFERENCES

1. USRDS, "US Renal Data System Annual Data Report 2011: Atlas of Chronic Kidney Disease and End-Stage Renal Disease in the United States, National Institutes of Health, National Institute of Diabetes and Digestive and Kidney Diseases, Bethesda, MD," 2011.
2. S. B. Park, J. K. Kim, and K.-S. Cho, "Complications of renal transplantation ultrasonographic evaluation," *Journal Of Ultrasound In Medicine*, vol. 26, no. 5, pp. 615–633, 2007.
3. A. Grabner, D. Kentrup *et al.*, "Non-invasive diagnosis of acute renal allograft rejection- Special focus on gamma scintigraphy and positron emission tomography," in *Current Issues and Future Direction in Kidney Transplantation*, 2013, ch. 4.
4. O. Wu, A. R. Levy *et al.*, "Acute rejection and chronic nephropathy: A systematic review of the literature," *Transplantation*, vol. 87, no. 9, pp. 1330–1339, 2009.
5. G. L. Myers, W. G. Miller *et al.*, "Recommendations for improving serum creatinine measurement: A report from the laboratory working group of the national kidney disease education program," *Clinical Chemistry*, vol. 52, no. 1, pp. 5–18, 2006.
6. E. L. W. Giele, *Computer methods for semi-automatic MR renogram determination*. Technische Universiteit Eindhoven, 2002.
7. J. Heaf and J. Iversen, "Uses and limitations of renal scintigraphy in renal transplantation monitoring," *Eur. J. Nucl. Med.*, vol. 27, no. 7, pp. 871–879, 2000.
8. H. Michaely, K. Herrmann *et al.*, "Functional renal imaging: Nonvascular renal disease," *Abdominal Imaging*, vol. 32, no. 1, pp. 1–16, 2007.
9. G. K. Von Schulthess, W. Kuoni *et al.*, "Semiautomated ROI analysis in dynamic MRI studies, Part II: Application to renal function examination," *J. Computer Assisted Tomogr.*, vol. 15, no. 5, pp. 733–741, 1991.
10. G. Gerig, R. Kikinis *et al.*, "Semiautomated ROI analysis in dynamic MRI studies: Part I: Image analysis tools for automatic correction of organ displacements," *IEEE Trans. Image Process.*, vol. 11, no. 2, pp. 221–232, 1992.
11. P. J. Yim, H. B. Marcos *et al.*, "Registration of time-series contrast enhanced magnetic resonance images for renography," in *Proc. the IEEE Symposium on Computer-Based Medical Systems (CMBS'01)*, vol. 1, Bethesda, MD, July 26–24, 2001, pp. 516–520.
12. J. A. de Priester, A. G. Kessels *et al.*, "MR renography by semiautomated image analysis: Performance in renal transplant recipients," *J. Mag. Reson. Imag.*, vol. 14, no. 2, pp. 134–140, 2001.
13. E. W. Giele, J. A. de Priester *et al.*, "Movement correction of the kidney in dynamic MRI scans using FFT phase difference movement detection," *J. Mag. Reson. Imag.*, vol. 14, no. 6, pp. 741–749, 2001.
14. E. Giele, "Computer methods for semi-automatic MR renogram determination," Ph.D. dissertation, Eindhoven University of Technology, Eindhoven, 2002.
15. H. K. Koh, W. Shen *et al.*, "Segmentation of kidney cortex in MRI studies using a constrained morphological 3D H-maxima transform," in *Proc. Int. Conf. Control, Automation, Robotics and Vision (ICARCV'06)*, Singapore, Dec. 26–29, 2006, pp. 1–5.
16. Y. Sun, M. P. Jolly, and J. M. F. Moura, "Integrated registration of dynamic renal perfusion MR images," in *Proc. Int. Conf. Image Process.*, Singapore, Oct. 24–27, 2004, pp. 1923–1926.
17. Y. Sun, "Registration and segmentation in perfusion MRI: Kidneys and hearts," Ph.D. dissertation, Carnegie Mellon University, Pittsburg, 2004.
18. Y. Sun, D. Yang *et al.*, "Improving spatiotemporal resolution of USPIO-enhanced dynamic imaging of rat kidneys," *Mag. Reson. Imag.*, vol. 21, no. 6, pp. 593–598, 2003.

19. Y. Sun, J. M. F. Moura, and C. Ho, "Subpixel registration in renal perfusion MR image sequence," in *Proc. Int. Symp. Biomed. Imaging*, Arlington, VA, April 15–18, 2004, pp. 700–703.
20. T. F. Chan and L. A. Vese, "Active contours without edges," *IEEE Trans. Image Process.*, vol. 10, no. 2, pp. 266–277, 2001.
21. H. E. Abdelmunim, A. A. Farag *et al.*, "A kidney segmentation approach from DCE-MRI using level sets," in *Computer Vision and Pattern Recognition Workshops, (CVPRW'08)*, vol. 1, Anchorage, Alaska, June 23–28, 2008, pp. 1–6.
22. S. E. Yuksel, A. El-Baz *et al.*, "A kidney segmentation framework for dynamic contrast enhanced magnetic resonance imaging," *J. Vibr. Control*, vol. 13, no. 9-10, pp. 1505–1516, 2007.
23. S. E. Yuksel, A. El-Baz, and A. A. Farag, "A kidney segmentation framework for dynamic contrast enhanced magnetic resonance imaging," in *Proc. International Symposium on Mathematical Methods in Engineering, (MME'06)*, Ankara, Turkey, April, 27Ű-29, 2006, p. 55Ű64.
24. A. El-Baz and G. Gimel'farb, "EM based approximation of empirical distributions with linear combinations of discrete Gaussians," in *Proc. Int. Conf. Image Process.*, vol. 4, San Antonio, Texas, USA, Sep. 16–19, 2007, pp. 373–376.
25. A. El-Baz, A. Elnakib *et al.*, "Precise segmentation of 3-D magnetic resonance angiography," *IEEE Trans. Biomed. Eng.*, vol. 59, no. 7, pp. 2019–2029, 2012.
26. A. El-Baz and G. Gimel'farb, "Robust medical images segmentation using learned shape and appearance models," in *Proc. Int. Conf. Medical Image Computing and Computer-Assisted Intervention*, London, UK, Sep. 20–24, 2009, pp. 281–288.
27. F. Khalifa, A. El-Baz *et al.*, "Non-invasive image-based approach for early detection of acute renal rejection," in *Proc. Int. Conf. Medical Image Computing and Computer-Assisted Intervention*, Beijing, China, Sep. 20–24, 2010, pp. 10–18.
28. F. Khalifa, G. M. Beache *et al.*, "Dynamic contrast-enhanced MRI-based early detection of acute renal transplant rejection," *IEEE Trans. Med. Imaging*, 2013.
29. ——, "Accurate automatic analysis of cardiac cine images," *IEEE Trans. Biomed. Eng.*, vol. 59, no. 2, pp. 445–455, 2012.
30. A. ElBaz, "Novel stochastic models for medical image analysis," Ph.D. dissertation, University of Louisville, Louisville, KY, USA, 2006.
31. A. Farag, A. El-Baz, and G. Gimel'farb, "Precise segmentation of multimodal images," *IEEE Trans. Image Process.*, vol. 15, no. 4, pp. 952–968, 2006.
32. O. Gloger, K. D. Tönnies *et al.*, "Prior shape level set segmentation on multistep generated probability maps of MR datasets for fully automatic kidney parenchyma volumetry," *IEEE Trans. Med. Imaging*, vol. 31, no. 2, pp. 312–325, 2012.
33. Y. Boykov and G. Funka-Lea, "Graph cuts and efficient N-D image segmentation," *Int. J. Computer Vis.*, vol. 70, no. 2, pp. 109–131, 2006.
34. H. Rusinek, Y. Boykov *et al.*, "Performance of an automated segmentation algorithm for 3D MR renography," *Mag. Reson. Med.*, vol. 57, no. 6, pp. 1159–1167, 2007.
35. A. M. Ali, A. A. Farag, and A. El-Baz, "Graph cuts framework for kidney segmentation with prior shape constraints," in *Proc. Int. Conf. Medical Image Computing and Computer-Assisted Intervention*, vol. 1, Brisbane, Australia, Oct. 29–Nov. 2, 2007, pp. 384–392.
36. A. El-Baz, S. E. Yuksel *et al.*, "2D and 3D shape based segmentation using deformable models," in *Medical Image Computing and Computer-Assisted Intervention–MICCAI'05*, 2005, pp. 821–829.
37. B. Chevaillier, D. Mandry *et al.*, "Functional segmentation of renal DCE-MRI sequences using vector quantization algorithms," *Neu. Process. Lett.*, vol. 34, no. 1, pp. 71–85, 2011.
38. T. Song, V. S. Lee *et al.*, "Four dimensional MR image analysis of dynamic renography," in *Proc. Conf. Eng. Med. Biol. Soc.*, New York, NY, Aug. 30–Sep. 3, 2006, pp. 3134–3137.
39. F. Zöllner, R. Sance *et al.*, "Assessment of 3D DCE-MRI of the kidneys using non-rigid image registration and segmentation of voxel time courses," *Computerized Med. Imag. and Graphics*, vol. 33, no. 3, pp. 171–181, 2009.
40. S. Li, F. G. Zöllner *et al.*, "Wavelet-based segmentation of renal compartments in DCE-MRI of human kidney: Initial results in patients and healthy volunteers," *Computerized Med. Imag. and Graphics*, vol. 36, no. 1, pp. 108–118, 2012.
41. X. Yang, P. Ghafourian *et al.*, "Nonrigid registration and classification of the kidneys in 3D dynamic contrast enhanced (DCE) MR images," in *Proc. SPIE Med. Imag.*, vol. 8314, 2012, pp. 1–9.

42. H. Wang, L. Dong *et al.*, "Validation of an accelerated demons algorithm for deformable image registration in radiation therapy," *Phy. Med. Biol.*, vol. 50, no. 12, pp. 2887–2905, 2005.
43. A. Farag, A. El-Baz *et al.*, "A framework for the detection of acute rejection with Dynamic Contrast Enhanced Magnetic Resonance Imaging," in *Proc. Int. Symp. Biomed. Imaging*, Virginia, USA, April, 2006, pp. 418–421.
44. A. El-Baz, G. Gimel'farb, and M. A. El-Ghar, "New motion correction models for automatic identification of renal transplant rejection," in *Proc. Int. Conf. Medical Image Computing and Computer-Assisted Intervention*, Brisbane, Australia, Oct. 29–Nov. 2, 2007, pp. 235–243.
45. A. El-Baz, A. Farag *et al.*, "Image analysis of renal DCE MRI for the detection of acute renal rejection," in *Proc. Int. Conf. Pattern Recognition*, Hong Kong, Aug. 20-Ű24, 2006, pp. 822–825.
46. ——, "A new CAD system for the evaluation of kidney diseases using DCE-MRI," in *Proc. Int. Conf. Medical Image Computing and Computer-Assisted Intervention*, 2006, pp. 446–453.
47. A. El-Baz, A. A. Farag *et al.*, "Application of deformable models for the detection of acute renal rejection," in *Deformable Models*, A. A. Farag and J. S. Suri, Eds., 2007, vol. 1, ch. 10, pp. 293–333.
48. G. Gimel'farb, A. Farag, and A. El-Baz, "Expectation-maximization for a linear combination of Gaussians," in *Proc. Int. Conf. Pattern Recognition*, 2004, pp. 422–425.
49. A. El-Baz, G. Gimel'farb, and M. A. El-Ghar, "A novel image analysis approach for accurate identification of acute renal rejection," in *Proc. Int. Conf. Image Process.*, 2008, pp. 1812–1815.
50. D. Zikic, S. Sourbron *et al.*, "Automatic alignment of renal DCE-MRI image series for improvement of quantitative tracer kinetic studies," in *Proc. SPIE Med. Imag.*, vol. 6914, 2008, pp. 1–8.
51. B. D. de Senneville, I. A. Mendichovszky *et al.*, "Improvement of MRI-functional measurement with automatic movement correction in native and transplanted kidneys," *J. Mag. Reson. Imag.*, vol. 28, no. 4, pp. 970–978, 2008.
52. A. Anderlik, A. Munthe-Kaas *et al.*, "Quantitative assessment of kidney function using dynamic contrast enhanced MRI-Steps towards an integrated software prototype," in *Proc. Int. Symp. Image Sig. Process. Anal. (ISPA'09)*, Salzburg, Austria, Sep. 16–18, 2009, pp. 575–581.
53. S. P. Sourbron, H. J. Michaely *et al.*, "MRI- measurement of perfusion and glomerular filtration in the human kidney with a separable compartment model," *IEEE Eng. Med. and Biol. Mag.*, vol. 43, no. 1, pp. 40–48, 2008.
54. F. Khalifa, M. A. El-Ghar *et al.*, "A comprehensive non-invasive framework for automated evaluation of acute renal transplant rejection using DCE-MRI," *NMR in Biomed.*, no. 2, 2013.
55. E. Hodneland, A. Kjorstad *et al.*, "In vivo estimation of glomerular filtration in the kidney using DCE-MRI," in *Proc. Int. Symp. Image Sig. Process. Anal. (ISPA'11)*, 2011, pp. 755–761.
56. V. Positano, I. Bernardeschi *et al.*, "Automatic 2D registration of renal perfusion image sequences by mutual information and adaptive prediction," *Mag. Reson. Materials in Phy., Biol. and Med.*, pp. 1–11, 2012.
57. A. El-Baz, G. Gimel'farb *et al.*, "Automatic analysis of 3D low dose CT images for early diagnosis of lung cancer," *Pattern Recognition*, vol. 42, no. 6, pp. 1041–1051, 2009.
58. A. El-Baz, F. Khalifa *et al.*, "A novel approach for global lung registration using 3D markov-gibbs appearance model," in *Proc. Int. Conf. Medical Image Computing and Computer-Assisted Intervention*, Nice, France, Oct. 1–5, 2012, pp. 114–121.
59. A. El-Baz, A. Soliman *et al.*, "Early assessment of malignant lung nodules based on the spatial analysis of detected lung nodules," in *Proc. Int. Symp. Biomed. Imaging*, 2012, pp. 1463–1466.
60. A. A. Farag, A. El-Baz *et al.*, "Appearance models for robust segmentation of pulmonary nodules in 3D LDCT chest images," in *Proc. Int. Conf. Medical Image Computing and Computer-Assisted Intervention*, Copenhagen, Denmark, Oct. 1–6, 2006, pp. 734–741.
61. F. Khalifa, G. M. Beache *et al.*, "State-of-the-art medical image registration methodologies: A survey," in *Handbook of Multi Modality State-of-the-Art Medical Image Segmentation and Registration Methodologies*, A. El-Baz, U. R. Acharya *et al.*, Eds., 2011, vol. 1, ch. 9, pp. 235–280.
62. D. Rueckert, M. J. Clarkson *et al.*, "Non-rigid registration using higher-order mutual information," in *Proc. SPIE Med. Imag.*, vol. 3979, 2000, pp. 438–447.
63. F. Khalifa, G. M. Beache *et al.*, "A new nonrigid registration framework for improved visualization of transmural perfusion gradients on cardiac first-pass perfusion MRI," in *Proc. Int. Symp. Biomed. Imaging*, 2012, pp. 828–831.
64. ——, "A new shape-based framework for the left ventricle wall segmentation from cardiac first-pass perfusion MRI," San Francisco, CA, April 7–11, 2013, pp. 41–44.